ACS OMEGA

http://pubs.acs.org/journal/acsodf

Article

Effects of Underground Coal Mining on Soil Spatial Water Content Distribution and Plant Growth Type in Northwest China

Kai Zhang,* Kang Yang, Xingtong Wu, Lu Bai, Jiangang Zhao, and Xinhui Zheng

Cite This: *ACS Omega* 2022, 7, 18688−18698

Read Online

ACCESS | Metrics & More | Article Recommendations

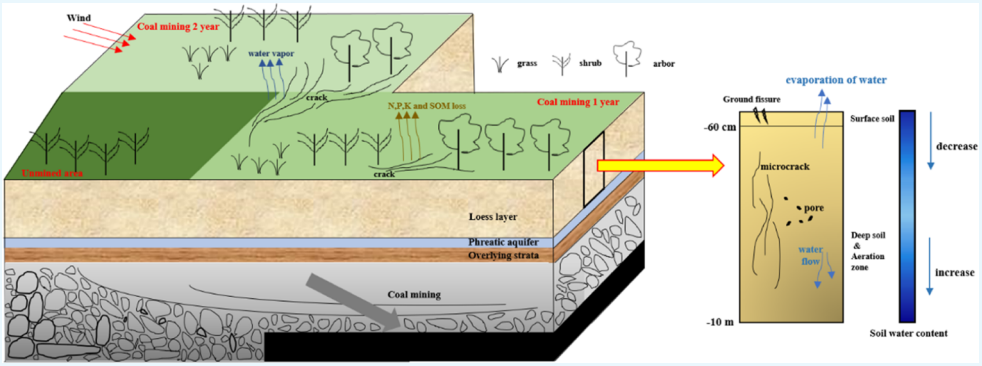

ABSTRACT: The impact of coal mining subsidence on surface ecology involves the influence of several ecological elements such as water, soil, and vegetation, which is systematic and complex. Given the unclear understanding of the synergistic change patterns of the water−soil−vegetation ecological elements in the influence of coal mining in the west, this paper investigates the impact of coal mining on the surface ecology, especially the distribution of soil water content (SWC). In 2020, this study collected 3000 soil samples from 60 sampling points (at depth of 0−10 m) and tested the SWC. All samples come from three different temporal and spatial areas of coal mining subsidence in the desert mining area of Northwest China where soil types are mainly aridisols. At the same time, the interactions among deep SWC and surface soil physical and chemical properties, surface SWC and soil fertility, and pH were analyzed. The spatial variability of soil moisture is reflected by kriging interpolation, and SWC values at different depths are predicted as a basis for monitoring the environmental impact of different coal mining subsidence years. The research has shown that the ground subsidence leads to a decrease in SWC value and changes in surface soil pH, physical and chemical properties, and covering vegetation, which have occurred from the beginning of coal mining. The impact of coal mining on the SWC of the unsaturated zone is mainly at the depth of 0−6 m, where SWC is not directly related to the nutrient content of the surface soil. The overall settlement of the ground will stir up simultaneous decline in the quality of deep SWC and topsoil. The findings of this investigation suggest that changes in the soil structure caused by coal mining subsidence are the key factor in SWC loss. Timely monitoring and repairing 0−6 m ground fissures, as well as selecting shrubs on the surface is the best choice for the restoration of the ecological environment and prevention of soil erosion in this area.

1. INTRODUCTION

In 2020, China's coal production reached 3.84 billion tons, accounting for 51% of the global output. As the largest coal producer and consumer for 30 consecutive years, coal mining plays an irreplaceable role in China's economic development, yet meanwhile it has caused serious negative impacts on the ecotope.[1] First, a large number of surface cracks formed at the edge of the subsidence area will destroy the original physical structure of the soil in the gas envelope, making the soil particles less homogeneous and fissures develop, causing evaporation and loss of soil moisture in the gas envelope;[2] second, soil nutrients will be lost during the development of fissures, causing a decrease in soil quality;[3] and finally, the water-conducting fissure zone formed downhole develops into the aquifer, converting part of the groundwater into mine water, causing a decrease in the groundwater level and waste of water resources.[4] High-intensity coal mining will break the dynamic balance between key ecological factors, such as surface topography, soil physical and chemical properties, moisture in the air pocket, and vegetation in local coal mining

Received: March 7, 2022
Accepted: May 10, 2022
Published: May 23, 2022

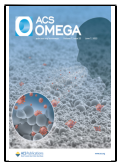

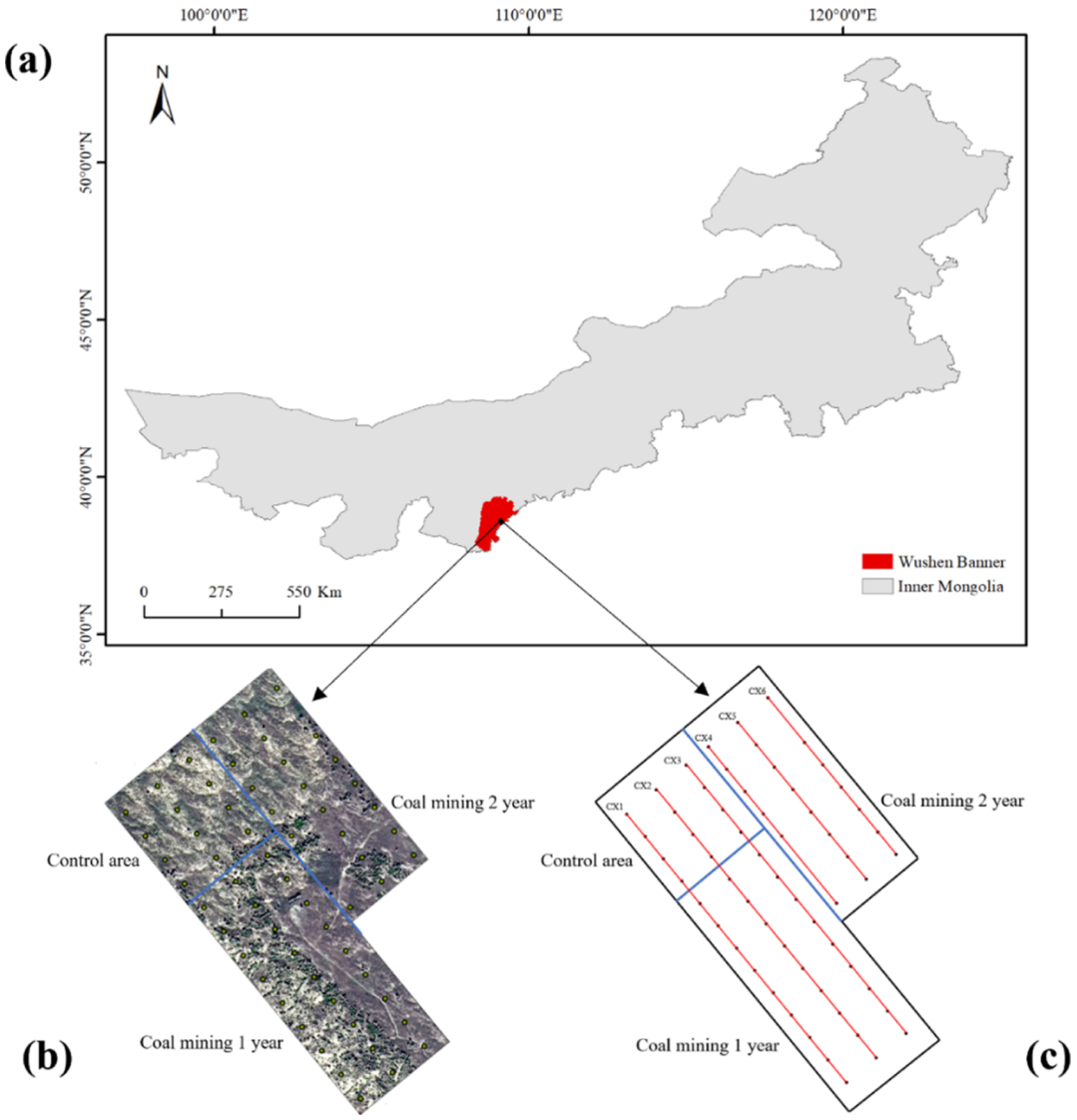

Figure 1. Image and schematics of the study site: (a) geographical location of the study site, (b) remote sensing aerial map, and (c) schematic diagram of the sampling layout.

subsidence areas, and cause a series of surface subsidence.[5] Shendong coalfield is located in a desert mining area in Northwest China. Through monitoring study on the dynamic surface subsidence,[6] it was found that high-intensity longwall mining speed can reach 9.0−13.3 m/day, and the maximum sedimentation speed in coalfield can reach 0.4 m/day, resulting in the annual decrease of the groundwater level.[7,8] From the perspective of a phreatic aquifer destruction mechanism, the surface subsidence will deform the rock layer in the goaf and strengthen the external force, causing the break and bend of overburden, which lead to the leakage and reduction of the phreatic level.[9] Aiming at the potential impacts of mining on ecology, human exploitation is considered as an extremely important factor in ecological deterioration and land degradation,[10] while unified opinion has not formed about the influence of phreatic level on soil water content (SWC). Therefore, understanding the influence principle of coal mining on the environment, especially the temporal and spatial variability of surface soil water distribution, is the basis and prerequisite for a reasonable and effective ecological restoration in the later stage.

The change of soil water is closely related to the migration and transformation of nutrients, and the fluctuation of moisture will trigger the change of nutrients such as N, P, K, and organic matter. As an important indicator of fertility, the nutrients of the soil determine the selection and growth of vegetation on the surface of the soil to a great extent. Similarly, the choice and survival of different types of vegetation will in turn affect the distribution of nutrients and water in the soil.[11,12] For example,[13] Guan compared the characteristics and changes of soil nutrient after the reclamation of the Loess Plateau mining area and found that the implementation of reclaiming measures among different types of land usage is the key to differences in topsoil nutrients. The hybrid model of trees, shrubs, and grasses is appropriate for ecological restoration in mine reclamation areas.[14] Presently, most research studies on the spatial variability of soil physical and chemical properties have focused on land reclamation and surface (0−1 m) soil. However, the variability information on soil properties in deep soil is necessary for the explanation and management of soil drainage, the leaching of nutrients and related research about groundwater,[15] while there are few

https://doi.org/10.1021/acsomega.2c01369
ACS Omega 2022, 7, 18688−18698

Table 1. Underground Coal Mining Data from Different Study Areas

	width (m)	depth (m)	thickness (m)	total volume (t)	progress (m)	intensity (t/m^2)
CMI	241.25	580.90	5.99	5.200×10^5	328.50	6.56
CMII	241.25	576.22	5.42	5.164×10^6	3034.60	7.05
CK						

reports on the correlation research studies between the soil in the vadose zone and the surface soil water in the coal mining subsidence area.

"The spatial interpolation methods include global interpolation, cubic spline function interpolation, distance reciprocal interpolation, kriging interpolation, and so forth. In contrast, the kriging model is suitable for situations with high spatial autocorrelation and dense sampling points, and its results are more accurate, but the data requirements are higher.[16] As a geostatistical model, kriging interpolation has been widely used for spatial prediction for both horizontal and vertical variability in soil properties.[17] Veronesi[18] used three-dimensional (3D) kriging combined variogram for mapping soil texture and compaction. 3D residual kriging could also be used to map soil organic carbon inventories.[19] Nevertheless, these approaches analyzing soil structure and properties, respectively, could not completely systematically clarify the impact of coal mining on SWC in subsidence areas of different ages. Thus, the kriging method is used in this study to analyze the influence mechanism of coal mining subsidence on the distribution of soil water to further verify the possible factors.

In this paper, soil samples collected from different subsidence areas of the no. 2 Nalinhe mine in Northwest China were tested for moisture as well as physical and chemical properties, including alkali hydrolyzable nitrogen (AN), available phosphorus (OP), available potassium (AK), soil organic matter (OM), and pH. The geostatistical analysis in ArcGIS 10.8 was used to simulate the 3D spatial distribution of soil moisture in the unsaturated zone and the surface layer, together with the analysis of soil physical and chemical properties and water correlation under different vegetation distributions, which could explain the influence of underground coal mining on the distribution of soil water in different subsidence areas. This study provides a reasonable and decisive spatial support for the recovery measures of soil water in the area with highly intensified coal mining subsidence disturbance.

2. MATERIALS AND METHODS

2.1. Study Area Description. The research area is located in the Southwest of the Ordos City in Inner Mongolia Province of China, which is a plateau desert and semi-desert area geographically ranging from 37°38′54″ to 39°23′50″ N, 108°17′36″ to 109°40′22″ E (Figure 1a). The mining area has a typical temperate continental monsoon climate, with tremendous temperature variation between day and night as well as no or little rain all around the year.[20] The annual average temperature is 6.8 °C, while the wind speed is 3.4 m/s, and the frost-free period is nearly 113−156 days. Moreover, the annual evaporation is 2200−2800 mm in the region, less than one-sixth of precipitation. The soil type is mainly fixed and semi-fixed aeolian sandy soil, generally growing xerophyte and semi-xerophyte vegetation. The phreatic water depth of the whole mining area is 19.15−25.65 m, while the average buried depth of the main coal seam is about 602 m.

Research location is the surface land in the eastern region of the second Nalinhe coalmine where underground coal mining activities were underway. The aerial view of the research site is obtained through remote sensing technology (Figure 1b). According to the real-time working conditions, control area (CK), area that has been mined for 1 year (CMI) and 2 years (CMII) were divided for this study, respectively. The size of the CK plot was 300 m × 300 m, with shrubland as the only type of vegetation. In addition to grassland, the plant types of CMI and CMII also include shrub and arbor forest land. Dimensions of two subsidence areas (CMI, CMII) are 200 m × 600 m and 300 m × 600 m, respectively, the underground coal mining is underway in CMI, while the ground subsidence was already in a stable period in CMII.

2.2. Sample Collection and Testing. According to the characteristics of underground coal mining face distribution, six survey lines were set up with equally spaced 100 m between the survey lines. The sampling points are evenly distributed along the survey line and at an interval of 75 m on both sides and the center of the roadway. GPS (NUI-T UT379A China, the positioning accuracy is better than 10 m, the speed measurement accuracy is better than 0.2 m/s, and the timing accuracy is better than 50 ns) was used to confirm and record the geographic coordinates of each sample point, and a total of 60 sample points were arranged, of which 12, 27, and 27 were in the CK, CMI, and CMII study areas (Figure 1c). Because the study area is flat, the plum blossom sampling method is suitable for collecting soil samples. At each sampling point, three composite samples were collected by a ring knife. Totally 1800 soil samples were collected at three depths of 10, 20, and 30 cm under the surface of the ground. The deep soil is separated by 0.5 m, among 20 layers total 1200 soil samples were drilled from 0.5 m underground to 10 m underground by using a Luoyang shovel. Each sample was measured in triplicate and all of them were weighed to test the SWC by measuring and calculating the average value. After mixing 10, 20, and 30 cm surface soil samples in equal proportions, the certified reference materials were used to determine the specimen's AN, OP, AK, OM, and pH.[21] The samples were collected from August 15 to August 22, 2022, and the sampling period was sunny with no rainfall occurring. According to the known monitoring data, coal mining has pumped away part of the groundwater, the groundwater loss rate of CK and CMI after coal mining is 0.76% compared to before, and the groundwater loss rate of CMII area is 0.78%; the ratio of mining depth to mining thickness is 97.03 for CMI, while CMII is 106.31. Specific information on coal mining is shown in Table 1.

2.3. Data Analysis Method. All data were statistically analyzed by SPSS20.0 software package, and the normal distribution test of the data was performed through the Kolmogorov−Smirnov (K−S) method. The Levene test was used to evaluate the homogeneity of variance. Maximum, minimum, mean, median, standard deviation (SD), and coefficient of variation (CV) were adopted as indicators to evaluate the impact of coal mining subsidence on soil water, of

https://doi.org/10.1021/acsomega.2c01369
ACS Omega 2022, 7, 18688−18698

which reliability has been verified in related research methods.[22]

Kriging insertion is also known as spatial local interpolation method which is based on the variogram theory and structural analysis.[23] Xu[24] researched on the spatial variation distribution of soil composition, and it was found that the 3D kriging interpolation method has the highest prediction accuracy. Using the known sample data in 3D space, the experimental semivariance function is constructed in the horizontal direction ($X-Y$ direction) and the vertical direction (Z direction). The calculation formula is as follows under the assumption of intrinsic stability

$$r(h) = \frac{1}{2N(h)} \sum_{i=1}^{N(h)} [Z(x_i) - Z(x_i + h)]^2$$

$Z(x_i)$ and $Z(x_i + h)$ are the sample values for $Z(x)$ at the point x_i and another point located in the distance h from the point x_i, respectively $[i = 1, 2, ..., N(h)]$, where h is the spatial distance between two points and $N(h)$ is defined the sample logarithm of all observation points, while the interval $r(h)$ is the semivariance function of the sample. When the data set has spatial autocorrelation, kriging interpolation can be used in this study is the following equation

$$Z(x_0) = \sum_{i=1}^{n} \lambda_i Z(x_i)$$

$Z(x_0)$ is the content of the soil water or other physical and chemical properties to be tested, n is the number of known samples around the point to be estimated, λ_i is the weight coefficients of each sample point, while the $Z(x_i)$ is the sample value at the ith sampling point. Krieger interpolation assumes that the data obey a normal distribution, but if the data do not obey a normal distribution, some data transformation is required to make them obey a normal distribution. The spatial distribution maps of soil water at different depths were created by the ArcGIS10.8 spatial interpolation.

3. RESULTS AND DISCUSSION

3.1. Content Characteristics of Soil Water and Physical−Chemical Properties. The SWC measured from each layer at 10 cm (H_{10}), 20 cm (H_{20}), and 30 cm (H_{30}) in the study area, as well as the overall pH, AN, OP, AK, and OM contents are shown in Table 2. The average SWCs from 10 to 30 cm soil depth are 3.92, 2.76, and 2.71%, which decreases with the increase of soil depth. In addition, the average value of H_{10} was 1.42 times higher than that of H_{20}, and the range of change from H_{20} to H_{30} is moderate, and the average value of H_{30} was 1.02 times lower than that of H_{20}. Therefore, the moisture content in the surface soil is very sensitive to changes in depth which can be used as a basis for judging the disturbance of the surface caused by coal mining subsidence.[25] The variations in pH were weak (CV < 0.1) and the data were more concentrated, implying that there was no significant difference in the pH of the soil in this area. Soil moisture content (H_{10}, H_{20}, and H_{30}) and physical and chemical properties (AN, OP, AK, and OM) showed pacific variation (0.1 < CV < 1), indicating that the obvious changes of these properties used to estimate the impact of underground coal mining was meaningful.

Table 2. Surface Soil Data Overview and Kolmogorov−Smirnov Inspection

	mean	SD	CV	min	max	P value
H_{10}	3.92	1.42	0.36	1.62	7.80	0.018
H_{20}	2.76	1.03	0.37	1.40	5.17	0.003
H_{30}	2.71	1.16	0.43	1.33	6.48	0.000
ln H_{10}						0.200
ln H_{20}						0.690
ln H_{30}						0.540
pH	7.26	0.14	0.02	6.91	7.51	0.200
AN	40.86	7.59	0.19	23.33	55.01	0.200
OP	21.14	3.82	0.18	12.07	27.54	0.200
AK	149.65	26.97	0.18	94.83	202.55	0.200
OM	15.90	3.01	0.18	9.14	23.56	0.200

The K−S test of (pH, AN, OP, AK, and OM) interpolation point a series of data shows that the data sets are all normally distributed (P > 0.05, confidence level 95%) except for SWC data. However, the logarithmic processing of H_{10}, H_{20}, and H_{30} passed the K−S test (Table 2), so the results of the comprehensive analysis revealed that kriging can be used for further data analysis.

Figure 2a shows that the surface SWC stepwise decreases with the augment of soil depth, and the overall variation tendency of the average water content in different subsidence areas was basically revealed as CK > CMI > CMII. The water content of CK decreases at first and then rises with the increase of depth of the soil layer, while the water content of the 20 cm depth in the unmined area was 67% lower than that of the 10 cm depth, but the value of the H_{30} is restored to 73% of H_{10}. Similarly, the CMI and CMII regions showed the same pattern, and it was noteworthy that the water content of the 2 year subsidence area was slightly higher than that of the 1 year subsidence district. Surface micro-cracks and subsidence will increase the infiltration rate and steady permeation rate of surface soil, which was not conducive to the maintenance of soil moisture.[26] With the extension of mining time, the soil moisture content in the subsidence area recovers faster,[27] and the measured data also showed that CMII has higher SWC than CMI, but not lower SWC in CMI and CMII than that in CK. The soil depths of 20 and 30 cm were disturbed by coal mining, so the water storage capacity decreases. Although the surface water storage performance has been restored to a certain extent with the increase of the year, presently it has not fully recovered to the unmined state. It can be inferred that underground coal mining is the main factor affecting the change of surface SWC, while the length of the subsidence year is a minor one. Given that the water content of the surface soil is affected by many factors, the distribution of surface vegetation and the physical and chemical properties of the soil are considered together to further verify the cross-influence caused by underground coal mining.

Figure 2b shows the distribution of deep SWC. The value of soil moisture at each depth had been tested by the K−S normal distribution test (P > 0.05, confidence level 95%). From the depth from 0.5 to 2 m, the SWC decreases with the growth of depth. There was no obvious rule for the change of SWC at the depth from 2.5 to 6 m, and the SWC gradually increases with the growth of soil depth below 6.5 m. Comparing with the same soil depth in the three regions, the CMI soil moisture variation degree is the highest (average CV is 43.6%), and the average soil water variation coefficients of the CK and CMII regions are 25.68 and 29.31%, respectively. The results show that the variation of soil moisture is decreased as the

https://doi.org/10.1021/acsomega.2c01369
ACS Omega 2022, 7, 18688−18698

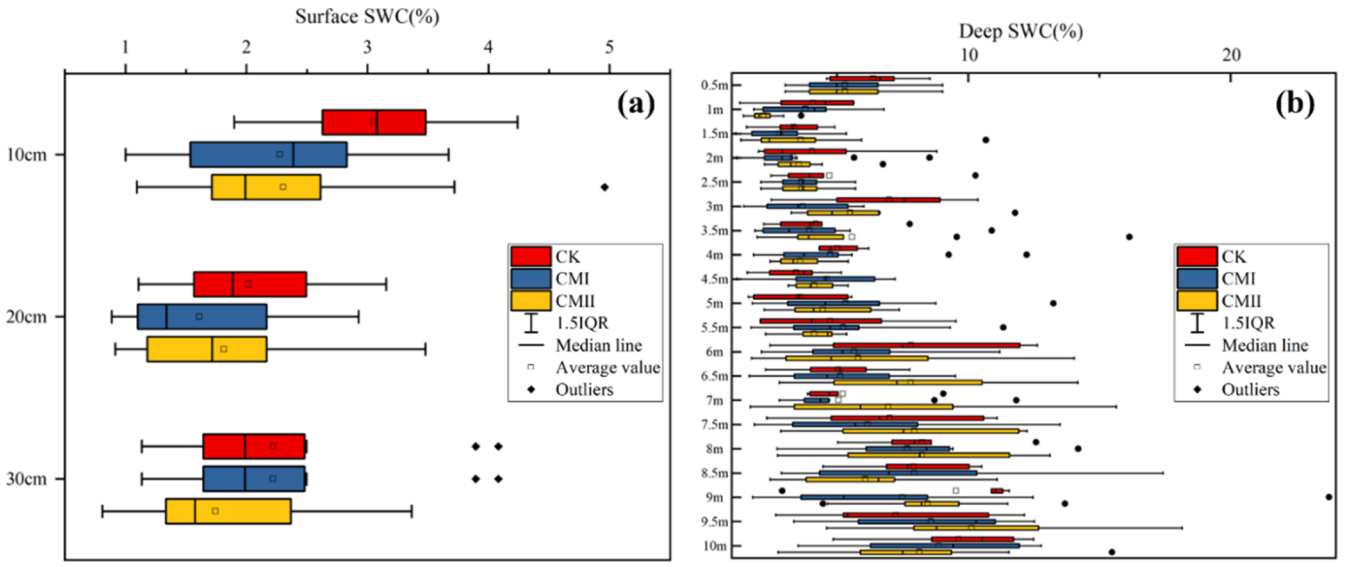

Figure 2. SWC of different depths: (a) surface SWC and (b) deep SWC.

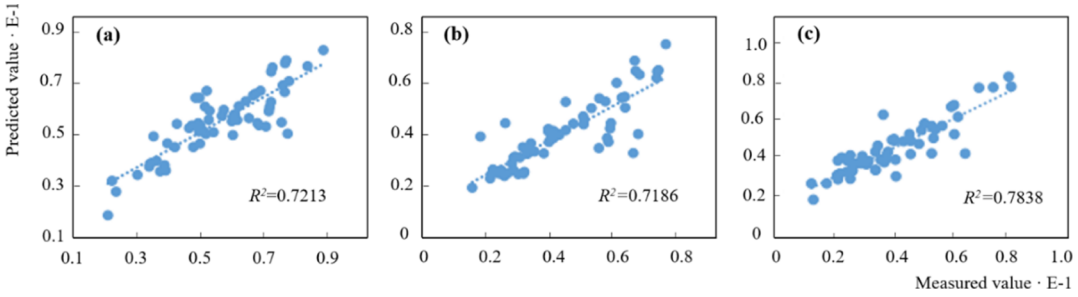

Figure 3. Cross-check charts: (a) H_{10}, (b) H_{20}, and (c) H_{30}.

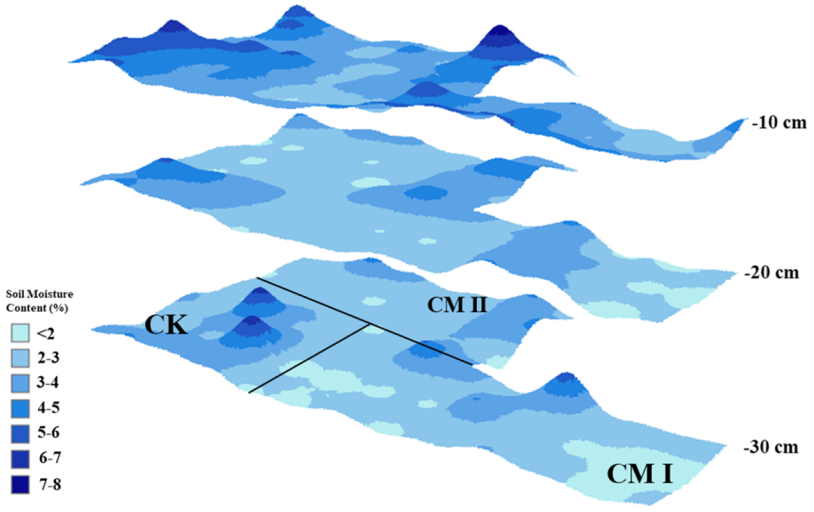

Figure 4. Spatial distribution of surface SWC.

subsidence entered a stable period caused by ground subsidence, and underground coal mining aggravated the fluctuation of deep SWC, which is consistent with the large fluctuations of surface SWC in the CMI region.

3.2. Simulation of Kriging Stratification of SWC. *3.2.1. Spatial Variability Structure of SWC.* As the key to spatial variation structure analysis, semi-variance analysis plays an important role in reasonably controlling the number of sampling points and improving interpolation accuracy. The standard for selecting the semivariance function model is under the maximum number of iterations. The smaller the results of the root mean squared error is, the better it is for the research. In this study, a spherical model was used to fit the spatial distribution of the moisture content of all soil layers, and the results of all values were tested by cross-validation ($R^2 > 0.7$) based on which a soil water distribution kriged map was formed and stretched in three dimensions.

https://doi.org/10.1021/acsomega.2c01369
ACS Omega 2022, 7, 18688−18698

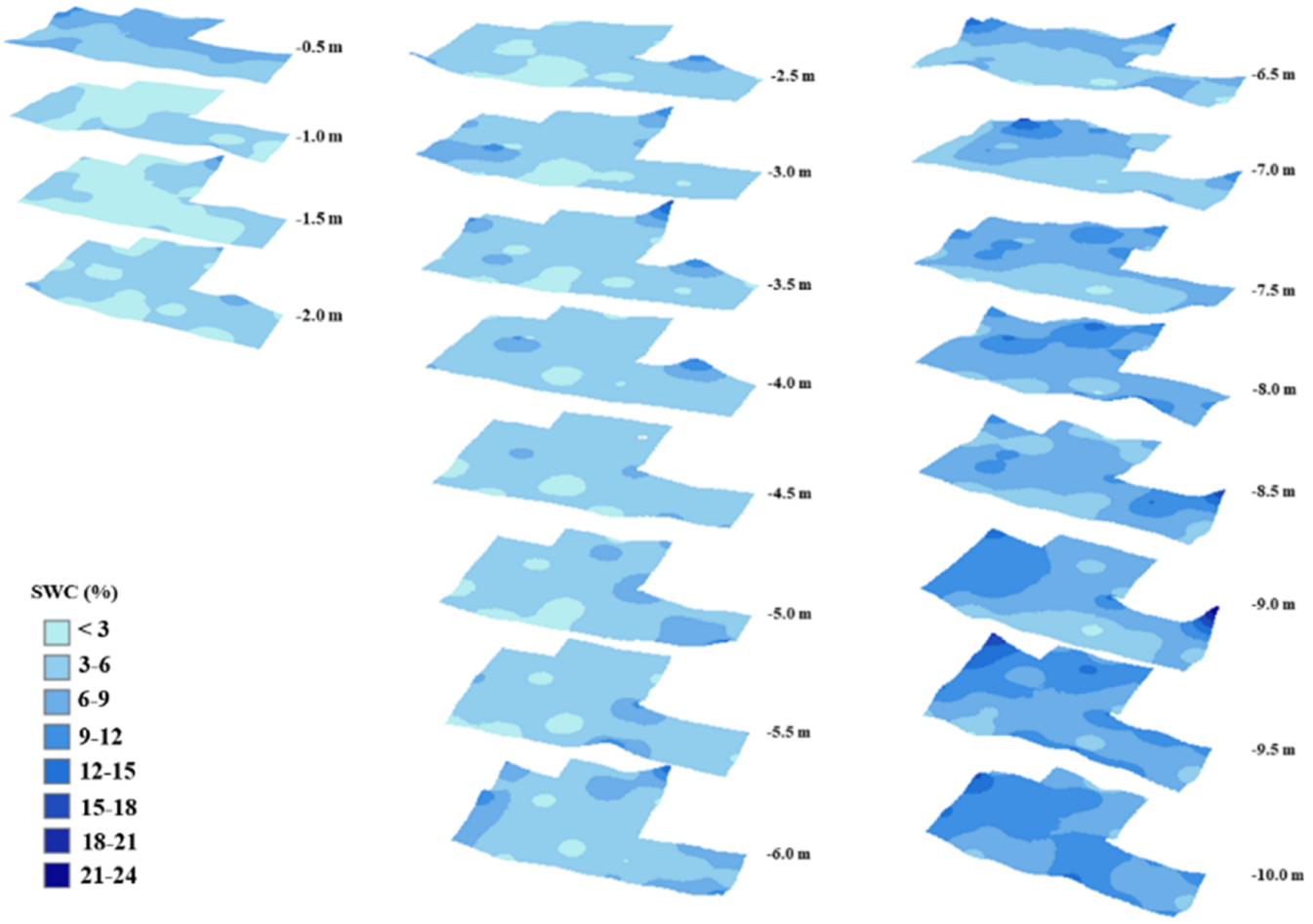

Figure 5. Spatial distribution of deep SWC.

Taking the establishment of the kriging model of surface soil water as the example, H_{10}, H_{20}, and H_{30} water content is best fitted with a spherical model, when the RMSE values are 0.003232, 0.001937, and 0.004130, and the R^2 values are 0.7213, 0.7186, and 0.7838, respectively (Figure 3). Moreover, there were no abnormal values in the data, indicating that the predictions are reliable and can be used to analyze the actual distribution of surface soil water.

3.2.2. Spatial Distribution of Surface SWC. Figure 4 shows the spatial distribution of SWC in three regions under different depths of soil. At the depth of 10 cm, the SWC is the highest in the central area of CK and the region with secondary high value is located in the southwest of CMI and the southeast of CMII, respectively. The SWC has experienced a significant decrease from CK to the surface subsidence area where the lowest value appeared in the adjacent position of the boundary of the three regions. The vegetation on the ground is sparsely distributed and the soil fertility is poor. Most of the soil nutrient content is lower in the sampling points of the marginal zone.[28] The static cracks on the surface cannot close by self-healing, which will increase the porosity of the soil, causing the vertical leakage of water and nutrients and damaging the roots of vegetation and reducing plants coverage.[29] Zhang[30] tracked and monitored the location of cracks at the Shendong coal mine and found that the SWC in the subsidence area was smaller than that in the unmined area, and the decline of ground fissures is particularly significant. From 0 to 90 cm depth, the water content shows a downward trend and the fluctuation ranges on 9.27−15.47%. Based on previous results, we can infer that the decrease of SWC in the transition from CK to subsidence area is caused by ground cracks.

CK area still has the highest SWC in the 20 cm depth soil layer. The water values in the southeast and northwest of CMI are low, where the plants distributed are mainly arbor plants. Correspondingly, shrubs are largely distributed in other regions. In the northwest of the CMII with sparse vegetation, the SWC value is also lower. Different vegetation types with diverse root distribution patterns will result in variational pore characteristics and soil structure.[31] The order of soil porosity under different plants coverage is arbor land > shrub forest > grassland.[32] Arbor tree-covered soils have greater porosity, confirming that different plant types also have an effect on the structure of the soil. Vegetation restoration will affect the loss of soil nutrients by changing the distribution of pores and preferential flow channels; in this case, reasonable vegetation configuration can reduce nutrient deprivation.[33] Therefore, shrubs are the best choice for subsidence area.

In the 30 cm depth soil layer, two high points of SWC appeared in the middle of the CK area. The value of CMI immediately decreased to the lowest when it transitioned to the southeast and the average values of SWC in the three regions are relatively close whose distribution shows a similar trend at a depth of 20 cm CK > CMII > CMI. It can be inferred that underground coal mining has a top-down and overall linkage effect on the water content of surface soil.

https://doi.org/10.1021/acsomega.2c01369
ACS Omega 2022, 7, 18688−18698

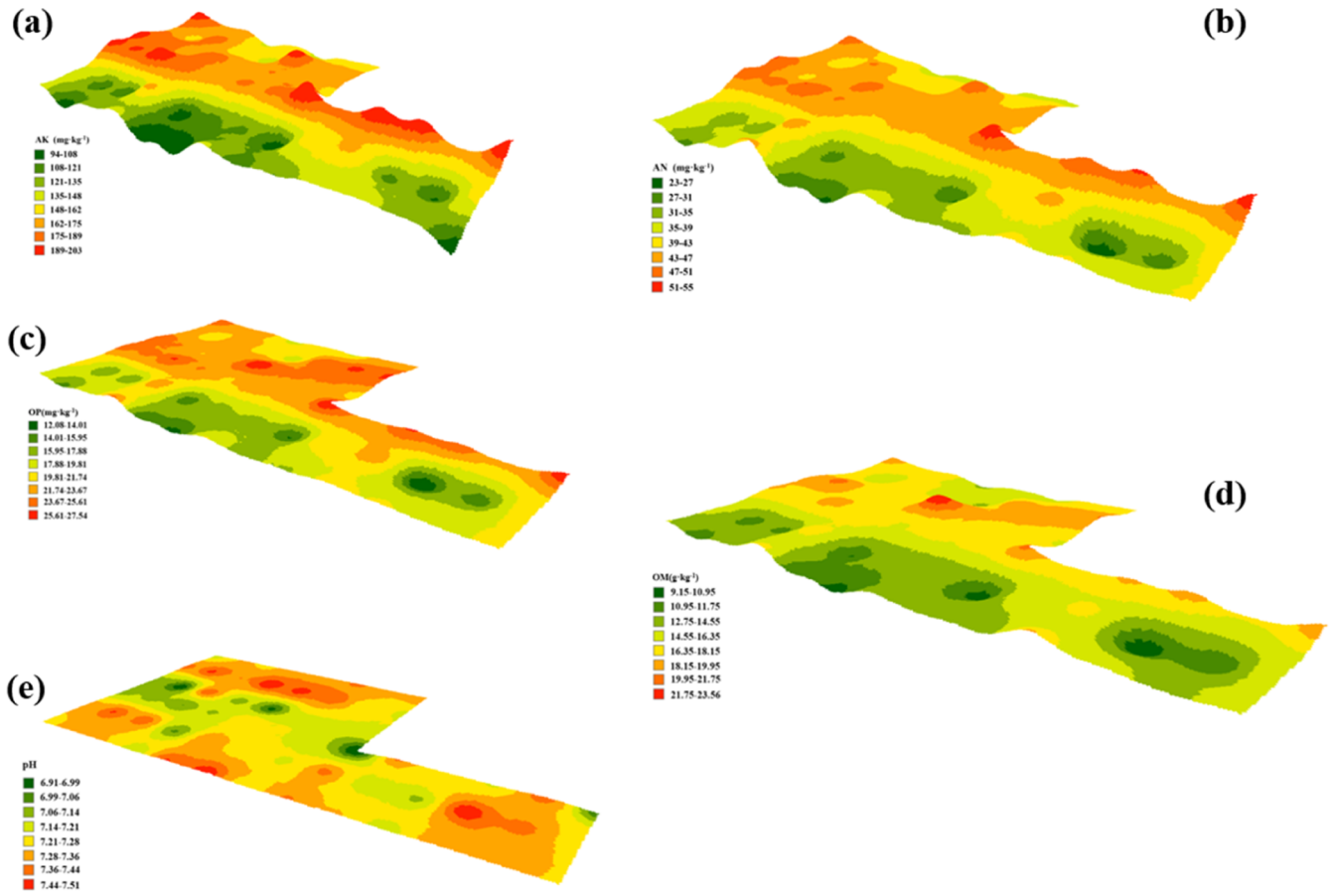

Figure 6. Spatial distribution of topsoil's physical−chemical properties: (a) AK, (b) AN, (c) OP, (d) OM, and (e) pH.

Table 3. Correlation Analysis of SWC and Soil pH[a]

		grassland			shrubland			arbor forest		
		H_{10}	H_{20}	H_{30}	H_{10}	H_{20}	H_{30}	H_{10}	H_{20}	H_{30}
CMI	pH	−0.475**	−0.415**	−0.317	0.258	−0.565**	−0.778**	−0.156	−0.188	−0.569**
CMII		−0.458**	−0.209	−0.273	−0.25	−0.238	−0.066	0.02	0.247	0.358*
CK					−0.094	0.361*	−0.278			

[a]* significant correlation at 0.05; ** is significantly correlated at the level of 0.01.

3.2.3. Spatial Distribution of Deep SWC. The distribution of deep SWC is generally $H_{6.5-10.0} > H_{0.5-2.0} > H_{2.5-6.0}$. Figure 5 shows that the area where each layer of soil transitions from CK to CMI has a significant decrease in water content. The surface SWC in the depth of 0.5−2 m continued the trend of gradual decline in topsoil as the depth decreased. Changes in soil texture had a strong influence on SWC,[34] as the soil particles gradually growing with the increase of depth during the deposition cycle, the soil particles show coarser, resulting in higher SWC of the upper soil than the deep soil.[35] In this study, only the CMI and CK regions $H_{0.5-2.0} > H_{2.5-6.0}$, while to depths below 6 m, the overall SWC began to stabilize. At depths below 6 m, the SWC gradually reaches a saturated and stable state. Akbariyeh found that the heterogeneity of the site soil is mainly manifested at the top soil down to 3 m from the surface, while the deeper soil matrix is a more uniform aquifer. However, the variation is only correlated with the fluctuation of the groundwater level.[36] It can be inferred that the fluctuation of $H_{6.5-10.0}$ is mainly affected by the surface subsidence and groundwater level decline caused by underground coal mining.

3.3. Relationship between SWC and Soil Physical−Chemical Properties under Different Vegetation Types. The overall decrease in soil nutrient values (AK, AN, OP, and OM) in CMI and CMII in the coal mining subsidence area can be seen from Figure 6. The low values of pH are mainly found in the adjacent locations of CK, CMI, and CMII, which confirms the influence of the possible ground fractures generated by coal mining subsidence on soil properties.

3.3.1. Interaction between Surface SWC and pH. Extensive studies have demonstrated that SWC and soil depth in arid and semi-arid regions were the most closely related environmental factors that restrict plant growth and the distribution of the microbial community structure.[37−39] Besides, soil pH is also considered to be the most important factor affecting biomass growth on the ground. A series of studies verified the conclusion in the northern Loess Plateau and even in global.[40] In this study, the correlation analysis between SWC and pH under the influence of different vegetations is shown in Table

https://doi.org/10.1021/acsomega.2c01369
ACS Omega 2022, 7, 18688−18698

Table 4. Correlation Analysis of SWC and Soil Fertility[a]

		grassland			shrubland			arbor forest		
		H_{10}	H_{20}	H_{30}	H_{10}	H_{20}	H_{30}	H_{10}	H_{20}	H_{30}
CMI	AN	−0.102	−0.006	0.190	−0.269	0.690**	0.638**	0.019	0.097	0.373**
	OP	−0.126	−0.008	0.236	−0.163	0.693**	0.787**	0.138	0.142	0.473**
	AK	−0.159	0.024	0.262	−0.189	0.637**	0.742**	0.032	0.252	0.425**
	OM	−0.175	−0.023	0.217	−0.109	0.664**	0.823**	0.242	0.296*	0.529**
CMII	AN	0.222	0.223	−0.224	0.276	0.340*	−0.170	0.191	−0.004	−0.194
	OP	−0.1777	0.496**	0.379*	0.311	0.470**	−0.157	0.416*	0.241	0.250
	AK	−0.029	0.324	0.056	0.387*	0.412*	−0.119	0.117	−0.004	−0.129
	OM	−0.153	0.433**	0.321	0.290	0.244	−0.278	0.270	0.114	0.175
CK	AN				0.380*	−0.423*	−0.004			
	OP				0.236	−0.474**	0.023			
	AK				0.307	−0.472**	0.005			
	OM				0.206	−0.469**	0.073			

[a]* significant correlation at 0.05; ** is significantly correlated at the level of 0.01.

Table 5. Pearson Correlations between the Soil Nutrients and Soil Water[a]

	AN	OP	AK	OM	pH	$H_{0.5-2.0}$	$H_{2.5-6.0}$	$H_{6.5-10}$
AN	1							
OP	0.930**	1						
AK	0.923**	0.900**	1					
OM	0.864**	0.966**	0.838**	1				
pH	−0.549**	−0.620**	−0.530**	−0.667**	1			
$H_{0.5-2.0}$	−0.542	−0.535	−0.471	−0.618	0.454	1		
$H_{2.5-6.0}$	−0.166	−0.167	0.110	−0.136	0.258	−0.353	1	
$H_{6.5-10.0}$	0.692**	0.686**	0.798**	0.636**	−0.601*	−0.355	0.345	1

[a]* significant correlation at 0.05; ** is significantly correlated at the level of 0.01.

3. In CMI, the value of H_{10}, H_{20}, and pH are significantly relevant to grassland, while the correlations are −0.475 and −0.415, which is a moderately negative correlation; similarly, H_{20}, H_{30}, and pH are significantly relevant to shrubland when the correlations are −0.565 and −0.778, respectively. H_{30} and pH are relevant in the arbor forest, and the correlation is −0.569 which is also a medium-degree correlation. In the CK and the CMII area, there is a slight correlation between water content and pH, and the rest is neither significant nor correlated. The pH of most areas is negatively correlated with the SWC because the content of H^+ increases with the rise of the moisture content, reducing the alkalinity value of the soil.[41] Therefore, the decrease of SWC in the mining area will cause the increase of pH. The changes of water content and pH are timely affected by the surface subsidence, grassland, and shrubland that are more sensitive to this fluctuation, whereas arbor woodland has relatively good stability.

3.3.2. Interaction between Surface SWC and Soil Fertility. The main source of water for surface plants is SWC, while soil fertility content is also an important factor affecting vegetation growth, so the relationship between SWC and vegetation types is interdependent and interactive.[42] SWC and physical−chemical properties of soil show different correlations under different vegetation types (Table 4), indicating that vegetation types have an important impact on soil properties, which in turn affects SWC.[43]

The correlation between SWC and soil fertility under the grassland distribution is relatively poor, while the SWC of the arbor forest merely at a depth of 30 cm below the CMI area shows a good relevance with the physical−chemical properties of the soil. In this research, shrubs are the only vegetation distributed in all regions, which demonstrates excellent correlation between the indicators in each region. In the CK area, H_{10}, H_{20}, and AN have weak correlations (correlation coefficients: 0.380 and −0.423); H_{20} and OP, AK, and OM also show the same regular (correlation coefficients: −0.474, −0.472, −0.469); the correlations between H_{20}, H_{30} and AN, OP, AK, and OM in CMI area are extremely significant (correlation coefficients: 0.690, 0.693, 0.637, and 0.664 and 0.638, 0.787, 0.742, and 0.823, respectively). H_{10} in the CMII region has a weak correlation with AK and the correlation coefficient is 0.387, while H_{20} has a similar discipline with AN, AK, and OP (correlation coefficients: 0.340, 0.412, and 0.470, respectively). It can be found that the correlation between SWC and soil fertility of shrubs on the area of CMI is the closest, which shows a positive correlation. Gao[44] found that *Caragana korshinskii* have outstanding drought tolerance as the roots can approach more water layers of soil, which causes conspicuous deep soil aridness in the stratum beyond the maximum penetration depth. Combining level ditches infiltration with holes on a slope could effectively enhance the SWC above the surface soil layer in shrubland and simultaneously cause fluctuations in the nutrient content above the 60 cm soil layer.[45] CMI is in the active period of underground coal mining where surface subsidence has caused changes in SWC and soil fertility values, which confirms that the interaction occurs at the beginning of subsidence.

3.3.3. Interaction between Deep SWC and Surface Soil Physical−Chemical Properties. Extracting coal seams in underground longwall mines would fracture overlying stratigraphy, in turn deteriorating aquifer connectivity and disturbing surface flows via subsidence disturbance,[46] which subsequently intensifies the variability of soil micropores and pore size distribution and impacts soil hydraulic characteristics and

https://doi.org/10.1021/acsomega.2c01369
ACS Omega 2022, 7, 18688−18698

nutrient availability.[47] Hou[48] built a numerical model to simulate the vertical flow, and it was found the storage-effect of the thick vadose zone could provide a persistent moisture downward flow below depth of 3 m where the groundwater recharge was steady. The deep SWC decreases first and then slowly rises, where the SWC from 2.5 to 6 m is in the transition zone with a lower value, which is consistent with the law of the vertical flow model of soil water. Given that the root systems of main herbaceous plants and floras were distributed in the range of 0−2 m in the research area,[5] researcher divided the deep soil into three profiles according to the gradient of 0.5−2.0 m ($H_{0.5-2.0}$), 2.5−6 m ($H_{2.5-6.0}$), and 6.5−10 m ($H_{6.5-10.0}$). Pearson's correlation analysis was taken to analyze the average value of the deep soil water and the surface soil water as well as physical−chemical properties at the corresponding points. It was found that only in the value of $H_{6.5-10}$, SWC showed a high degree of positive correlation with the physical−chemical properties of the surface soil (AN, OP, AK, OM, and pH) (Table 5).

As the most important discharge method of groundwater, phreatic evaporation refers to the process of shallow groundwater moving upward in the unsaturated zone and contributing to land surface evapotranspiration.[49] When the buried depth of groundwater exceeds a certain level, the evaporation approaches zero, and this critical length is the limitary buried depth of the phreatic water. The external evaporation capacity (temperature, wind speed, and light) and soil water transport capacity (soil texture, structure, water content, and vegetation coverage) are the main influential factors.[50] Zhang[51] pointed out that the phreatic evaporate limitation of burial depth ranged from 2.38 to 5.16 m from sandy gravel to loam. According to the observation data of groundwater evaporation in the arid area of Northwest China, the maximum buried depth of table water aquifer is less than 4.5 m.[52] From experimental results, the 6.5−10 m deep underground soil has exceeded the ultimate depth of phreatic evaporation, which has no direct impact on the physical−chemical properties of the surface soil. The best explanation for the significant positive correlation of the values is that underground coal mining leads to the settlement of the ground as a whole, which causes a simultaneous decrease in the physical−chemical values of deep soil water and surface soil.

4. CONCLUSIONS

The study made an analysis of the influence of the physical and chemical properties of the soil moisture and topsoil from earth surface to 10 m after the incident of surface subsidence induced by underground coal mining. Vertically, it has shown that SWC in all regions reflected a trend of decreasing before increasing with the deepening of soil depth. Horizontally, the study presents that the SWC of the CK is always higher than that of the subsidence area shaped by coal mining. The SWC content at all depths will decrease significantly when transitioning from the unmined area to subsidence area; overall, the 1 year subsidence area has the highest variation coefficient of soil moisture (the average value is 43.6%). As the subsidence enters a stable period, the 2 year subsidence area reflects a reduced variation, which is still higher than that of the CK. Such being the case, it is inferred that ground fissures and micropores caused by coal mining subsidence gives a clear explanation of this phenomenon. The changes in the water content, pH, and nutrients of the lower layer soil of different vegetation types will be affected by ground subsidence and have occurred from the beginning of the ground subsidence. In coal mining subsidence areas, shrubs can be preferred as the main plants for land reclamation. There is no direct correlation between deep SWC ($H_{6.5-10}$) and surface soil nutrients, while the overall settlement of the ground will cause the simultaneous decline of deep soil water and surface soil quality.

In summary, the changes of surface soil subsidence and micro-structure stem from underground coal mining. Furthermore, the deformed soil structure can be self-healing with the extension of the post-mining time. Timely landfill can be taken to treat surface subsidence and cracks in view of the affected depth of SWC in the unsaturated zone ranging from 0 to 6 m. Meanwhile, planting shrubs in coal mining subsidence areas is a good option for reducing soil moisture loss. In this way, the impact of mining on the phreatic level is reduced and the stability of the ecological environment of the coal mining area can be maintained.

AUTHOR INFORMATION

Corresponding Author

Kai Zhang − *School of Chemical &Environmental Engineering, China University of Mining and Technology, Beijing 100083, China;* orcid.org/0000-0001-7735-7663; Phone: +86-010-62339810; Email: zhangkai@cumtb.edu.cn

Authors

Kang Yang − *School of Chemical &Environmental Engineering, China University of Mining and Technology, Beijing 100083, China;* orcid.org/0000-0002-0776-0921

Xingtong Wu − *School of Chemical &Environmental Engineering, China University of Mining and Technology, Beijing 100083, China*

Lu Bai − *School of Chemical &Environmental Engineering, China University of Mining and Technology, Beijing 100083, China*

Jiangang Zhao − *School of Chemical &Environmental Engineering, China University of Mining and Technology, Beijing 100083, China*

Xinhui Zheng − *School of Chemical &Environmental Engineering, China University of Mining and Technology, Beijing 100083, China*

Complete contact information is available at: https://pubs.acs.org/10.1021/acsomega.2c01369

Notes

The authors declare no competing financial interest.

ACKNOWLEDGMENTS

This work was supported by the Research on Ecological Restoration and Protection of Coal Base in Arid Eco-fragile Region (GJNY2030XDXM-19-03.2); the Yue Qi Young Scholar Project, China University of mining and Technology (Beijing) (2019QN08); and the National Key Research and Development Program of China (2018YFC0406404).

REFERENCES

(1) CNCA (China National Coal Association). *2020 Annual Report on the Development of the Coal*; CNCA: Beijing, 2020.report

(2) Wang, Q.; Dong, S.; Wang, H.; Yang, J.; Wang, X.; Zhao, C.; Zhang, X. Influence of mining subsidence on soil water movement law and its regulation in blown-sand area of Western China. *J. China Coal Soc.* **2021**, *46*, 1532−1540.

(3) Cheng, W.; Bian, Z.-f.; Dong, J.-h.; Lei, S.-g. Soil properties in reclaimed farmland by filling subsidence basin due to underground coal mining with mineral wastes in China. *Trans. Nonferrous Metals Soc. China* **2014**, *24*, 2627−2635.
(4) Ma, X.; Fan, L.; Zhang, X.; Li, W.; Zhang, H. Water-preserved mining based on relationship between vegetation and groundwater. *J. China Coal Soc.* **2017**, *42*, 1277−1283.
(5) Yang, Y.; Erskine, P. D.; Zhang, S.; Wang, Y.; Bian, Z.; Lei, S. Effects of underground mining on vegetation and environmental patterns in a semi-arid watershed with implications for resilience management. *Environ. Earth Sci.* **2018**, *77*, 605.
(6) Xu, J.; Zhu, W.; Xu, J.; Wu, J.; Li, Y. High-intensity longwall mining-induced ground subsidence in Shendong coalfield, China. *Int. J. Rock Mech. Min. Sci.* **2021**, *141*, 104730.
(7) Nakayama, T. Simulation of complicated and diverse water system accompanied by human intervention in the North China Plain. *Hydrol. Process.* **2011**, *25*, 2679−2693.
(8) Sun, S.; Qiu, L.; He, C.; Li, C.; Zhang, J.; Meng, P. Drought-Affected Populus simonii Carr. Show Lower Growth and Long-Term Increases in Intrinsic Water-Use Efficiency Prior to Tree Mortality. *Forests* **2018**, *9*, 564.
(9) Liu, S.; Li, W. Zoning and management of phreatic water resource conservation impacted by underground coal mining: A case study in arid and semiarid areas. *J. Clean. Prod.* **2019**, *224*, 677−685.
(10) Dai, W.; Dong, J.; Yan, W.; Xu, J. Study on each phase characteristics of the whole coal life cycle and their ecological risk assessment-a case of coal in China. *Environ. Sci. Pollut. Res.* **2017**, *24*, 1296−1305.
(11) Dey, P.; Karwariya, S.; Bhogal, N. Spatial Variability Analysis of Soil Properties Using Geospatial Technique in Katni District of Madhyapradesh, India. *Int. J. Plant Soil Sci.* **2017**, *17*, 1−13.
(12) Liu, J.; Sui, Y.; Yu, Z.; Shi, Y.; Chu, H.; Jin, J.; Liu, X.; Wang, G. High throughput sequencing analysis of biogeographical distribution of bacterial communities in the black soils of northeast China. *Soil Biol. Biochem.* **2014**, *70*, 113−122.
(13) Guan, Y.; Zhou, W.; Bai, Z.; Cao, Y.; Huang, Y.; Huang, H. Soil nutrient variations among different land use types after reclamation in the Pingshuo opencast coal mine on the Loess Plateau, China. *Catena* **2020**, *188*, 104427.
(14) Fang, X.; Xue, Z.; Li, B.; An, S. Soil organic carbon distribution in relation to land use and its storage in a small watershed of the Loess Plateau, China. *Catena* **2012**, *88*, 6−13.
(15) Zhang, Y.; Ji, W.; Saurette, D. D.; Huq, E. T.; Li, H.; Shi, Z.; Viacheslav, A.; Asim, B. Three-dimensional digital soil mapping of multiple soil properties at a field-scale using regression kriging. *Geoderma* **2020**, *366*, 114253.
(16) Abedini, M. J.; Nasseri, M.; Ansari, A. Cluster-based ordinary kriging of piezometric head in West Texas/New Mexico-Testing of hypothesis. *J. Hydrol.* **2008**, *351*, 360−367.
(17) Li, J.; Heap, A. D. A review of comparative studies of spatial interpolation methods in environmental sciences: Performance and impact factors. *Ecol. Inf.* **2011**, *6*, 228−241.
(18) Veronesi, F.; Corstanje, R.; Mayr, T. Mapping soil compaction in 3D with depth functions. *Soil Tillage Res.* **2012**, *124*, 111−118.
(19) Poggio, L.; Gimona, A. National scale 3D modelling of soil organic carbon stocks with uncertainty propagation - An example from Scotland. *Geoderma* **2014**, *232*, 284−299.
(20) Xu, D.; Song, A.; Tong, H.; Ren, H.; Hu, Y.; Shao, Q. A spatial system dynamic model for regional desertification simulation - A case study of Ordos, China. *Environ. Model. Software* **2016**, *83*, 179−192.
(21) Pang, X.-Y.; Bao, W.-K.; Zhang, Y.-M. Evaluation of soil fertility under different Cupressus chengiana forests using multivariate approach. *Pedosphere* **2006**, *16*, 602−615.
(22) Chen, T.; Chang, Q.; Liu, J.; Clevers, J. G. P. W. Spatio-temporal variability of farmland soil organic matter and total nitrogen in the southern Loess Plateau, China: a case study in Heyang County. *Environ. Earth Sci.* **2016**, *75*, 28.
(23) Zhang, K.; Qiang, C.; Liu, J. Spatial distribution characteristics of heavy metals in the soil of coal chemical industrial areas. *J. Soils Sediments* **2018**, *18*, 2044.
(24) Xu, D. *Spatial Variability and 3D Simulation of Soil Organic Matter and Total Nitrogen at Different Scales*; Institutes of Technology of Henan, 2016.
(25) Wang, J.; Qin, Q.; Bai, Z. Characterizing the effects of opencast coal-mining and land reclamation on soil macropore distribution characteristics using 3D CT scanning. *Catena* **2018**, *171*, 212−221.
(26) Wang, J. Influence of Coal Mining Subsidence on Physical and Chemical Properties of Sandy Soil in Semi-Arid Area. Master's Theses, Inner Mongolia Agricultural University, 2007.
(27) Zhang, Y. *Effects of Coal Mining on Soil Environment and Microbial Restoration in Western Area of China*; China University of Mining & Technology: Beijing, 2016.
(28) Guo, J.; Zhang, Y.; Huang, H.; Yang, F. Deciphering soil bacterial community structure in subsidence area caused by underground coal mining in arid and semiarid area. *Appl. Soil Ecol.* **2021**, *163*, 103916.
(29) He, Y.; He, X.; Liu, Z.; Zhao, S.; Bao, L.; Li, Q.; Yan, L. Coal mine subsidence has limited impact on plant assemblages in an arid and semi-arid region of northwestern China. *Ecoscience* **2017**, *24*, 91−103.
(30) Zhang, Y.; Bi, Y.; Chen, S. L.; Wang, J.; Han, B. Effects of Subsidence Fracture Caused by Coal-mining on Soil Moisture Content in Semi-arid Windy Desert Area. *Environ. Sci. Technol.* **2015**, *38*, 11−14.
(31) Pei, Y.; Huang, L.; Li, D.; Shao, M. a. Characteristics and controls of solute transport under different conditions of soil texture and vegetation type in the water−wind erosion crisscross region of China's Loess Plateau[J]. *Chemosphere* **2021**, *273*, 129651.
(32) Zhang, M.; Fang, L. Accumulation and transport of nutrients in agricultural sandy soils. *J. Soil Water Conserv.* **2006**, *20*, 46−49.
(33) Zhang, B.; Yang, Y.-s.; Zepp, H. Effect of vegetation restoration on soil and water erosion and nutrient losses of a severely eroded clayey Plinthudult in southeastern China. *Catena* **2004**, *57*, 77−90.
(34) Arredondo, T.; Delgado-Balbuena, J.; Huber-Sannwald, E.; Garcia-Moya, E.; Loescher, H. W.; Aguirre-Gutierrez, C.; Rodriguez-Robles, U. Does precipitation affects soil respiration of tropical semiarid grasslands with different plant cover types. *Agric. Ecosyst. Environ.* **2018**, *251*, 218−225.
(35) Sun, L.; Chang, X.; Yu, X.; Jia, G.; Chen, L.; Wang, Y.; Liu, Z. Effect of freeze-thaw processes on soil water transport of farmland in a semi-arid area. *Agric. Water Manag.* **2021**, *252*, 106876.
(36) Akbariyeh, S.; Bartelt-Hunt, S.; Snow, D.; Li, X.; Tang, Z.; Li, Y. Three-dimensional modeling of nitrate-N transport in vadose zone: Roles of soil heterogeneity and groundwater flux. *J. Contam. Hydrol.* **2018**, *211*, 15−25.
(37) Che, R.; Deng, Y.; Wang, F.; Wang, W.; Xu, Z.; Hao, Y.; Xue, K.; Zhang, B.; Tang, L.; Zhou, H.; Cui, X. Autotrophic and symbiotic diazotrophs dominate nitrogen-fixing communities in Tibetan grassland soils. *Sci. Total Environ.* **2018**, *639*, 997−1006.
(38) Shi, P.; Zhang, Y.; Hu, Z.; Ma, K.; Wang, H.; Chai, T. The response of soil bacterial communities to mining subsidence in the west China aeolian sand area. *Appl. Soil Ecol.* **2017**, *121*, 1−10.
(39) Wang, B.; Wang, Y.; Cui, X.; Zhang, Y.; Yu, Z. Bioconversion of coal to methane by microbial communities from soil and from an opencast mine in the Xilingol grassland of northeast China. *Biotechnol. Biofuels* **2019**, *12*, 236.
(40) Tripathi, B. M.; Stegen, J. C.; Kim, M.; Dong, K.; Adams, J. M.; Lee, Y. K. Soil pH mediates the balance between stochastic and deterministic assembly of bacteria. *ISME J.* **2018**, *12*, 1072−1083.
(41) Shi, P.; Zhang, Y.; Hu, Z.; Ma, K.; Wang, H.; Chai, T. Spatio-temporal Variation of Farmland Soil pH and Associated Affecting Factors in the Past 30 Years of Shandong Province, China. *Acta Pedol. Sin.* **2020**, *58*, 180−190.
(42) Zhang, J.; Jin, L. Relationship between soil moisture dynamics and climatic factors in temperate meadow steppe in Ewenki

https://doi.org/10.1021/acsomega.2c01369
ACS Omega 2022, 7, 18688−18698

Autonomous Banner of Inner Mongolia. *Anim. Husb. Feed Sci.* **2019**, *40*, 75−79.
(43) Peng, S.; Chen, A.; Fang, H.; Wu, J.; Liu, G. Effects of vegetation restoration types on soil quality in Yuanmou dry-hot valley, China. *Soil Sci. Plant Nutr.* **2013**, *59*, 347−360.
(44) Gao, X.; Zhao, X.; Li, H.; Guo, L.; Lv, T.; Wu, P. Exotic shrub species (Caragana korshinskii) is more resistant to extreme natural drought than native species (Artemisia gmelinii) in a semiarid revegetated ecosystem. *Agric. For. Meteorol.* **2018**, *263*, 207−216.
(45) Wang, K.; Zhang, X.; Ma, J.; Ma, Z.; Li, G.; Zheng, J. Combining infiltration holes and level ditches to enhance the soil water and nutrient pools for semi-arid slope shrubland revegetation. *Sci. Total Environ.* **2020**, *729*, 138796.
(46) Mason, T. J.; Krogh, M.; Popovic, G. C.; Glamore, W.; Keith, D. A. Persistent effects of underground longwall coal mining on freshwater wetland hydrology. *Sci. Total Environ.* **2021**, *772*, 144772.
(47) Ma, K.; Zhang, Y.; Ruan, M.; Guo, J.; Chai, T. Land Subsidence in a Coal Mining Area Reduced Soil Fertility and Led to Soil Degradation in Arid and Semi-Arid Regions. *Int. J. Environ. Res. Publ. Health* **2019**, *16*, 3929.
(48) Hou, L.; Wang, X.-S.; Hu, B. X.; Shang, J.; Wan, L. Experimental and numerical investigations of soil water balance at the hinterland of the Badain Jaran Desert for groundwater recharge estimation. *J. Hydrol.* **2016**, *540*, 386−396.
(49) Li, H.; Wang, W.; Liu, B. The daily evaporation characteristics of deeply buried phreatic water in an extremely arid region. *J. Hydrol.* **2014**, *514*, 172−179.
(50) Pei, Y.; Huang, L.; Li, D.; Shao, M. A. Characteristics and controls of solute transport under different conditions of soil texture and vegetation type in the waterewind erosion crisscross region of China's Loess Plateau. *Chemosphere* **2021**, *273*, 129651.
(51) Zhang, Y. Calculation of unsteady groundwater flow during pumping of group Wells. *Groundwater Unsteady Flow Calculation and Groundwater Resources Evaluation*; Wuhan University Press, 2013.
(52) Fan, Z.; Chen, Y.; Ma, Y.; Li, H.; Kurban, A.; Abdimijit. Determination of suitable depth of ecological groundwater in arid area of northwest China. *J. Arid Environ.* **2008**, *22*, 1−5.

https://doi.org/10.1021/acsomega.2c01369
ACS Omega 2022, 7, 18688−18698